

# Combination Paclitaxel and Laser-Activated NanoTherapy for Inducing Cell Death in Head and Neck Squamous Cell Carcinoma

Gee Young Lee<sup>1,2</sup>, Mohamed Mubasher<sup>3</sup>, Brian P. Pollack<sup>4,5</sup>, Tamra McKenzie<sup>1,4</sup>, Maya B. Cothran<sup>6</sup>, Hadiyah N. Green<sup>1,2,6\*</sup>

<sup>1</sup>Department of Surgery, Morehouse School of Medicine, 720 Westview Drive, Atlanta, GA 30310, USA; <sup>2</sup>Biomedical Laboratory Research & Development Service, Department of Veterans Affairs, Office of Research and Development, Birmingham VA Medical Center, 700 19th Street, Birmingham, AL 35233, USA; <sup>3</sup>Community Health and Preventive Medicine, Morehouse School of Medicine, 720 Westview Drive, Atlanta, GA 30310, USA; <sup>4</sup>Atlanta VA Medical Center, Atlanta VA Health Care System, 1670 Clairmont Road, Decatur, GA 30033, USA; <sup>5</sup>Department of Dermatology, Emory University, 1525 Clifton Road, Suite 100, Atlanta, GA 30322, USA; <sup>6</sup>Ora Lee Smith Cancer Research Foundation, Advanced Technology and Development Center, 75 5th Street NW, Atlanta, GA 30308, USA

## ABSTRACT

Combination, adjuvant, and neoadjuvant therapies have been emerging as practical approaches to increase the efficacy of lower drug doses, decrease side effects, and improve overall survival outcomes, especially for patients with difficult-to-treat tumors. Our work focuses on combining paclitaxel (PTX) with Laser-Activated NanoTherapy (LANT) as an adjuvant therapy to enhance the therapeutic efficacy of lower doses of PTX for treating head and neck squamous cell carcinoma (HNSCC). The results demonstrated the potential of the PTX and LANT combination for treating HNSCC using three cell lines: Detroit 562, FaDu, and CAL 27. The 1 nM PTX+5 nM LANT combination was the most effective treatment for all cell lines, showing up to 89.8% of cell death in CAL 27. The 1 nM PTX+5 nM LANT combination also produced the greatest PTX dose reduction for Detroit 562 and CAL 27, resulting in an 86.0% and 86.8% decrease, from the 7.1 nM and 7.6 nM of PTX monotreatment respectively. For FaDu, the 0.5 nM PTX+5 nM combination had the greatest dose reduction, resulting in an 80.8% decrease, from the 2.6 nM of PTX monotreatment. The results suggest that LANT may boost the therapeutic efficacy of low doses of PTX and induce the same percentage of cell death as high doses of PTX monotreatment. Therefore, these in vitro findings may lower PTX dosages and lead to improved patient outcomes.

**Keywords:** Paclitaxel; Dose reduction; Combination therapy; Laser-activated nanotherapy

## INTRODUCTION

Paclitaxel (PTX), more commonly known as Taxol® (Bristol-Myers Squibb), is one of the most effective broad-spectrum chemotherapeutic drugs approved to treat several cancers including breast, ovarian, pancreatic, lung, and Kaposi's sarcoma [1,2]. As an anti-cancer plant alkaloid, part of the taxane family, PTX is known for its cytotoxic effect of microtubule stabilization [3]. Usage of PTX in off-label treatment is also widely practiced for a variety of other cancer types including that of the head and neck [2]. Specifically, head and neck squamous cell carcinoma (HNSCC) has a poor prognosis with a 5-year survival rate of less than 50%, globally [4-6]. PTX would be more effective as standard of care for HNSCC but many patients present with locally advanced, drug resistant tumors

or may not tolerate the side effects of chemotherapy and radiation [4-8]. Consequently, new approaches are required to address the unmet need of the many HNSCC patients with a poor prognosis.

The clinical applications and efficacy of PTX for treating HNSCC and other cancer types has been limited by numerous factors including severe side effects and inadequate pharmacodynamic parameters. The poor water solubility of PTX is also a persistent issue restricting PTX usage. Due to this property, PTX injection solution contains ethanol and Cremophor EL that affect the cellular uptake and increase adverse effects like anaphylactic reactions [1,2,9]. In addition, PTX has side effects that commonly include neutropenia, hair loss, peripheral neuropathy, and pain [3,10-12]. Manipulating the dosing schedule, limiting the dose, and combining PTX with other treatment modalities help to improve

\*Correspondence to: Hadiyah N Green, Department of Surgery, Morehouse School of Medicine, 720 Westview Drive, Atlanta, GA 30310, USA, Tel: 1 4047521682; E-mail: hgreen@msm.edu

Received: December 27, 2020; Accepted: January 25, 2021; Published: January 28, 2021

Citation: Lee GY, Mubasher M, Pollack BP, McKenzie T, Cothran MB (2021) Combination Paclitaxel and Laser-Activated NanoTherapy for Inducing Cell Death in Head and Neck Squamous Cell Carcinoma. J Nanomed Nanotech. 12: 557.

Copyright: ©2021 Lee GY, et al. This is an open-access article distributed under the terms of the Creative Commons Attribution License, which permits unrestricted use, distribution, and reproduction in any medium, provided the original author and source are credited.

patient tolerance by decreasing the toxicity burden [10,13-15]. Currently, the optimal clinical dosage depends on cancer type and it is typical to be followed by cisplatin. The FDA has approved the general administration for single-agent PTX at 175 mg/m<sup>2</sup> for 3 h infusion every 3 weeks [16,17]. Side effects have been found to be dose-related, with higher doses resulting in higher frequency, prompting the exploration of new delivery measures including combination therapies and dose reductions [1-3,18].

PTX has been combined with nanoparticles and nanomaterials primarily to improve drug delivery and efficacy to circumvent the poor solubility profile and to enhance tumor targeting [1,19,20]. Exploring the anti-cancer potential of nanoparticles and nanomaterials as agents of transdermal drug delivery [21], radiotherapy [22], and photothermal or photodynamic therapy [23-25] has demonstrated dramatic improvement in tumor targeting, therapeutic efficacy, and drug dose reduction. In our previous studies, we employ photothermal therapy (PTT) utilizing gold nanoparticles and NIR light, showing great success in tumor treatment *in vitro* and *in vivo* as a site-specific ablative approach rather than theranostic drug delivery [26]. We use near-infrared excitation of gold nanorods (AuNRs), called as Laser-Activated NanoTherapy (LANT). Our novel LANT alone has demonstrated greater than 95% cell death *in vitro* ( $p < 0.0001$ ) and greater than 95% tumor regression *in vivo* ( $p < 0.0001$ ) [26,27].

In this study, we combine PTX with LANT to provide a synergistic cells death at a decreased PTX dosage. LANT presents an opportunity to override some of the biological obstacles encountered within the tumor microenvironment such as PTX solubility, permeability, and stability. To our knowledge, no such platform has been approved by the FDA for use in humans. As a result, we investigated how LANT, as part of an adjuvant therapy regimen, can enhance the therapeutic efficacy of lower doses of PTX for treating three head and neck squamous cell carcinoma (HNSCC) cell lines, Detroit 562, FaDu, and CAL 27.

## MATERIAL AND METHODS

### Materials

Gold (III) chloride trihydrate (HAuCl<sub>4</sub>), cetyltrimethylammonium bromide (CTAB), sodium borohydride (NaBH<sub>4</sub>), silver nitrate (AgNO<sub>3</sub>), L-ascorbic acid, potassium carbonate (K<sub>2</sub>CO<sub>3</sub>) and

dimethyl sulfoxide (DMSO) were purchased from Sigma-Aldrich (St. Louis, MO). Thiol-terminated methoxy poly(ethylene glycol) (mPEG-SH, MW 5,000K) and PTX were purchased from Creative PEGWorks (Winston-Salem, NC) and Selleck Chemicals (ImClone Systems, New York, NY), respectively. UltraPure water (18 MΩ) was used for AuNR preparation.

### Cell Lines

Three human HNSCC cell lines were used for this study: a human pharyngeal carcinoma cell line, Detroit 562, and two human squamous cell carcinoma cell lines, FaDu and CAL 27. The cell lines were purchased from the American Type Culture Collection (ATCC, Manassas, VA). Upon receiving the cell lines from ATCC, the passage number was set at one, and passage 3-7 of each cell line was used. Cells tested negative for mycoplasma. The HNSCC cell lines were cultured in Dulbecco's Modified Eagle Medium (Gibco) containing 10% v/v heat-inactivated fetal bovine serum (Corning), supplemented with 4.5 g/L glucose, L-glutamine, and penicillin-streptomycin (Corning) and incubated at 37°C in a 5% CO<sub>2</sub> humidified atmosphere.

### Preparation of AuNRs

AuNRs were fabricated by the seed-mediated growth at 25°C using a freshly prepared aqueous solution according to our previously described method [26]. Briefly, their outer CTAB layer was replaced with mPEG-SH in order to increase the biocompatibility of the AuNRs, as shown in Figure 1A and the PEGylated AuNRs solution was centrifuged at 7,600×g for 20 min at 25°C and re-dispersed in deionized water to remove excess CTAB and non-specifically bound mPEG-SH molecules. The PEGylated AuNRs were characterized by a Hitachi HF2000 STEM (aberration-corrected dedicated Scanning Transmission Electron Microscope) to verify consistency in shape and size (left in Figure 1B) and a Mettler Toledo UV/VIS Spectrophotometer UV5Nano to determine the 808 nm absorption peak (right in Figure 1B). One AuNR was 40 nm in length and 10 nm in width, thus providing the aspect ratio, R=4 and the concentration of AuNRs solution was calculated using Beer-Lambert Law based on the molar absorptivity,  $\epsilon = 5 \times 10^9 \text{ L} \cdot \text{mol}^{-1} \cdot \text{cm}^{-1}$  for 808 nm and aspect ratio, R=4 [28]. Our LANT platform works by shining a harmless laser light at 808 nm (laser activation) on cancer cells in the culture medium containing AuNRs. The laser light instigates electron oscillations inside the

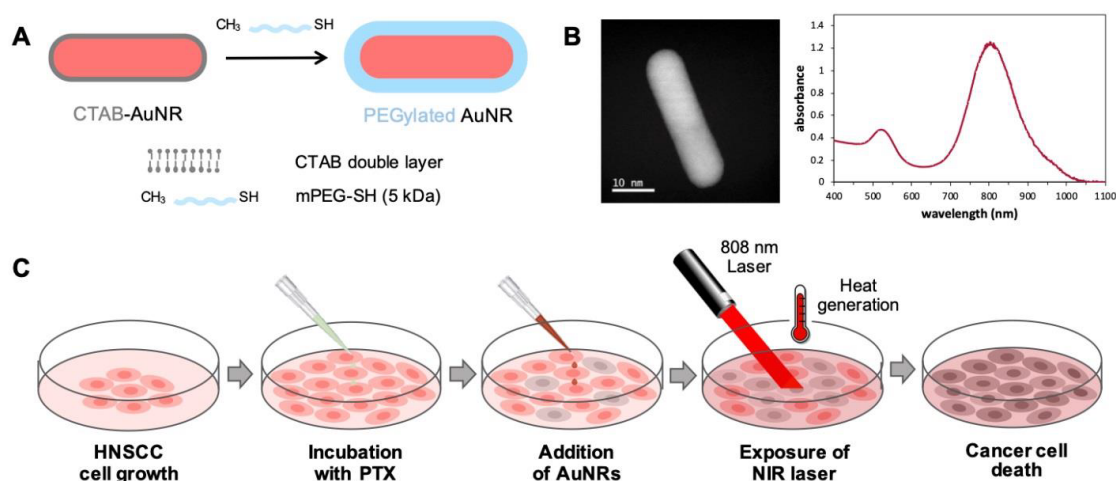


**Figure 1:** (A) Structure of PEGylated AuNRs utilized in Laser-Activated NanoTherapy (LANT), (B) 808 nm absorption peak and transmission electron microscopy (TEM) image of a AuNR, 40 nm in length and 10 nm in width, aspect ratio (R=4), and (C) schematic illustration of PTX and LANT combination treatment *in vitro*.

AuNRs that generate heat and the consequent heat gets transferred to the surrounding cancer cells, providing a local, thermal death for the cancer cells. Figure 1C illustrates the schematic method of PTX and LANT combination treatment *in vitro*.

### Cell Death by LANT Monotreatment

A total of  $6 \times 10^4$  cells/well were seeded in 96-well culture plates and treated at approximately 100% confluence. Cells were divided into 4 groups: no treatment, laser only (no addition of AuNRs), AuNRs only (no laser treatment), and LANT to demonstrate the potent cell death ability of LANT. AuNRs (25  $\mu$ L) at 25 nM were added to AuNRs only and LANT groups. We previously determined that 25 nM of AuNRs was the most effective concentration. All groups excluding the no treatment group were exposed to a diode near-infrared (NIR) laser (Information Unlimited, Amherst, NH, USA) with 808 nm wavelength at 1.875 W/cm<sup>2</sup> (spot size around 4 mm) for 4 min. Within 5 min after laser excitation, the cell viability was determined by the Presto Blue Assay. Briefly, the culture medium containing AuNRs as removed and replaced with the culture medium containing Presto Blue™ Cell Viability Reagent (10% v/v, Thermo Fisher Scientific). The cells were incubated at 37°C for 30 min. The plate was read at a 560/590 nm excitation/emission wavelength using the Spectra Max® M5 Microplate Reader (Molecular Devices, Sunnyvale, CA, USA). The fluorescence reading of the blank was subtracted from all samples. Test sample fluorescence readings were divided by the control and multiplied by 100 to give the percentage of cell viability. Then, the percentage of cell death was calculated by subtracting the percentage of cell viability from 100% (see formula below).

$$\% \text{ of cell death} = 100 - \% \text{ cell viability} = 100 - \left( \frac{\text{fluorescence of sample} - \text{fluorescence of blank}}{\text{fluorescence of control} - \text{fluorescence of blank}} \right) \times 100$$

### Cell Death by PTX Monotreatment

Cells were seeded in 96-wells plates at  $1 \times 10^4$  cells/well and allowed to adhere overnight. The culture medium was then replaced with a fresh medium containing PTX at various concentrations, 0.01-40 nM, and cells were incubated at 37°C for 48 h. The percentage of cell death was also determined by the PrestoBlue Assay, as described above.

### Combination of PTX and LANT *in vitro*

HNSCC cell lines were seeded in 96-wells plates at  $1 \times 10^4$  cells/well and allowed to adhere overnight. The culture medium was then replaced with fresh medium containing PTX at two concentrations (0.5 nM or 1 nM), and cells were incubated with PTX at 37°C for 48 h. Immediately after the 48-h incubation, the medium containing PTX was removed, and the cells were washed with PBS once. Then 25  $\mu$ L of AuNRs in PBS at the concentration of 2.5 nM or 5 nM were added onto the PTX-treated cells and exposed to 4 min of 808 nm wavelength NIR irradiation at 1.875 W/cm<sup>2</sup>. As described above, the cell viability induced by the PTX + LANT combination treatment was evaluated using the Presto Blue Assay immediately after LANT treatment and then the final percentage of cell death was calculated. Each treatment combination was performed in quadruplicate (n = 4), and the results are expressed as the mean  $\pm$  standard deviation.

### Calculations for EC50 and PTX Monotreatment Dose Reduction

The half-effective concentrations (EC50) of PTX and LANT for the 3 HNSCC cell lines were calculated with the EC50 calculator

provided by AAT Bioquest® using the Four-Parameter Logistic (4PL) model [29] and then the dose reduction realized by combining PTX with LANT was estimated by comparing the combination treatment to the monotreatment.

### Statistical Power and Analysis

The total sample size for the regression analyses was 72 (four observations per each of the six treatments (n=6) and three cell lines. We assumed (1) an Ordinary Least Square multiple regression model with the treatment by cell lines as predictors, (2) an assumed R<sup>2</sup> value of 0.7 for the full model (proportion of variability in percent cell death explained by the treatment by cell combinations), (3) a differential effect in R<sup>2</sup> of 0.025 for each treatment by cell line combination, and (4) overall 0.05 significance level. Consequently, there is at least 90% resulting power in the model to detect a statistically significant difference between at least eight comparisons of the combination of PTX and LANT versus the corresponding PTX monotreatment. Cell death percentages across the six treatment conditions, by cell line, were summarized by mean and standard deviations, median (min and max). Comparisons in percent cell death between treatment combinations by cell lines were undertaken using Linear Mixed Model (LMM) regression modeling approach with interaction (between treatment and cell lines) terms. Multiple comparisons were adjusted using the Bonferroni correction, with an overall nominal statistical significance of  $\alpha=0.05$ . No sigmoid (non-linear) feature for data was detected since all of the percent data lies between 17-95. However, given the bounded nature of the percent data (between 0 and 100), LMM results were also confirmed using a two-limit Tobit model [29,30]. The comparisons of interest for this study are those between PTX alone treatments (i.e., 0.5 nM PTX and 1 nM PTX) and the treatments involving a combination of the PTX and LANT (i.e., 0.5 nM PTX+2.5 nM LANT; 0.5 nM PTX+5 nM LANT; 1 nM PTX+2.5 nM LANT; and 1 nM PTX+5 nM LANT). Summaries and differences were plotted using Boxplots to relay distributional differences by treatment and cell lines. All analyses used SAS 9.4 and R statistical software (R Core Team, 2019).

## RESULTS

### Effects of LANT and PTX monotreatments

LANT monotreatment is an interaction of the NIR laser and AuNRs that causes an increase in local temperatures, resulting in a tailored and site-specific cellular death. We compared LANT monotreatment with several control groups: no treatment, and laser only, and AuNRs. As shown in Figure 2, the LANT monotreatment with 25 nM of AuNRs induced greater than 98% cell death for three HNSCC cell lines, Detroit 562, FaDu, and CAL 27. Only the LANT treatment group showed significant cell death in all cell lines compared to the no treatment, laser only, and AuNRs only showing 0%, less than 3%, and less than 10%, respectively. Neither the laser nor the AuNR-solution caused cell death without the other; they have to work together to effectively kill the intended cells.

The percentage of cell death and dose response curve induced by PTX monotreatment for HNSCC is illustrated in Figure 3. The PTX concentration was directly proportional to the percentage of cell death. However, administering the high PTX doses necessary to achieve a complete therapeutic response after 48 h in humans

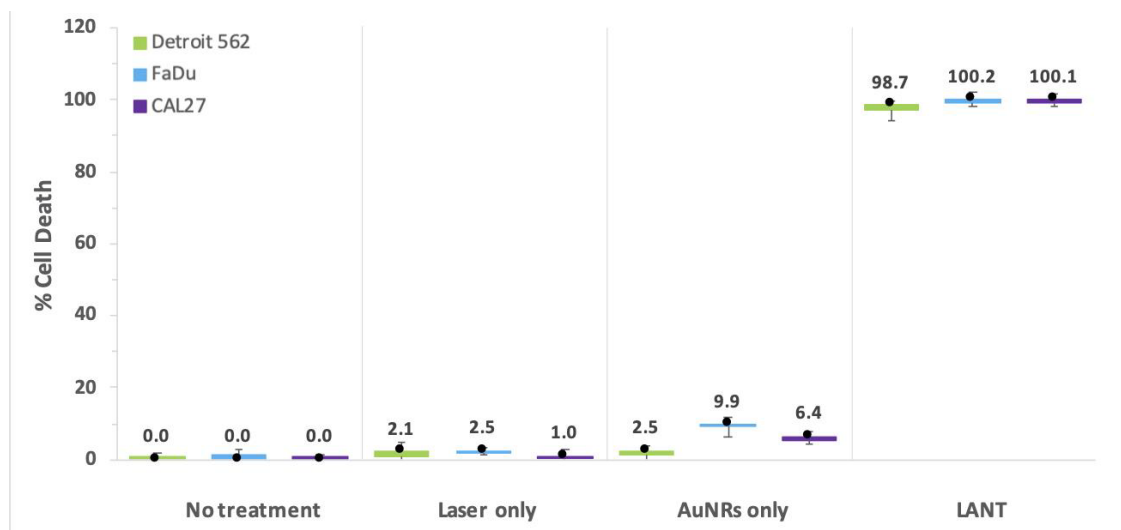


**Figure 2:** Box and whisker plot to display the ability of LANT monotreatment to induce cell death, compared to the no treatment, laser only (no addition of AuNRs), and AuNRs only (no laser treatment), for HNSCC cell lines: Detroit 562 (green bar), FaDu (blue bar), and CAL 27 (purple bar). The concentration of AuNRs in PBS (25  $\mu$ L) was 25 nM to generate the maximum cell death. Boxes (whiskers) indicate variability outside the upper and lower quartiles of  $n=6$  and dots show the mean values of  $n=6$ .

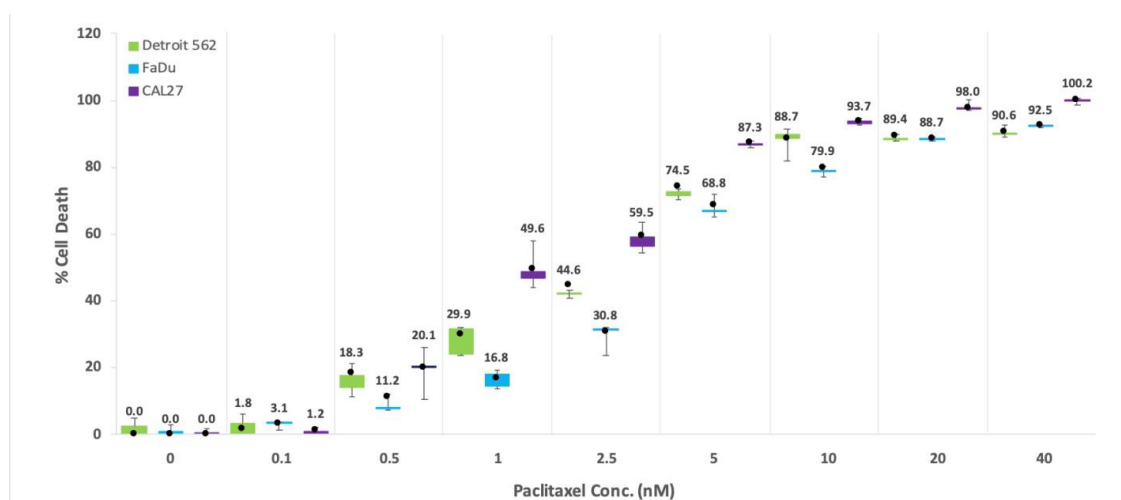


**Figure 3:** Box and whisker plot to display PTX monotreatment dose-response with PTX concentration for HNSCC cell lines: Detroit 562 (green bar), FaDu (blue bar), and CAL 27 (purple bar). Boxes (whiskers) indicate variability outside the upper and lower quartiles of  $n=6$  and dots show the mean values of  $n=6$ .

would result in patient intolerance due to increased severe side effects and toxicity. CAL 27 was the most sensitive to PTX and FaDu was the least sensitive to PTX. In this study, 40 nM of PTX resulted in approximately 100% cell death in CAL 27, and 91% and 93% cell death in Detroit 562 and FaDu, respectively, during the 48-h treatment window. The EC<sub>50</sub> values of LANT for each cell line, determined in our previously study, were 8.08 nM, 11.03 nM and 6.68 nM, respectively; and the EC<sub>50</sub> values of PTX for each cell line were 2.18 nM, 3.38 nM and 1.36 nM, respectively (Table 1).

### Combination of PTX and LANT treatments

The PTX and LANT monotreatment EC<sub>50</sub> values in Table 1 informed the low dose selections for the combination experiments for both PTX and LANT. To delineate and emphasize the efficacy of the PTX+LANT combination treatment, 0.5 and 1 nM of PTX were used in the combination treatment as they were the concentrations that induced less than 50% cell death for all cell lines. Likewise, 2.5 and 5 nM of AuNRs for LANT were selected as they were also the concentrations that induced less than 50% cell death for all cell lines. The percentage of cell death due to the

**Table 1:** EC<sub>50</sub> values for LANT and PTX monotreatments. LANT and PTX monotreatment concentrations resulted in the EC<sub>50</sub> values for three HNSCC cell lines: Detroit 562, FaDu and CAL 27.

EC <sub>50</sub>	Cell Lines		
	Detroit 562	FaDu	CAL 27
LANT (nM)	8.08	11.03	6.68
PTX (nM)	2.18	3.38	1.36

four PTX+LANT combination treatments, (PTX at 0.5 nM or 1 nM)+(LANT at 2.5 nM or 5 nM), was significantly higher than that due to the two PTX monotreatments (0.5 nM or 1 nM) for all three HNSCC cell lines, Detroit 562, FaDu, and CAL 27 (Figure 3).

### Summary statistics and LMM regression Post-Hoc results

Based on the cell death percentage data shown in Figure 4, the descriptive statistics, mean percentage (Mean), and standard deviation (SD) were summarized for the six treatment groups and three cell lines in Table 2. The LMM regression test compared the means of the six treatment groups for three cell lines. There was a statistically significant difference in the means of most groups.



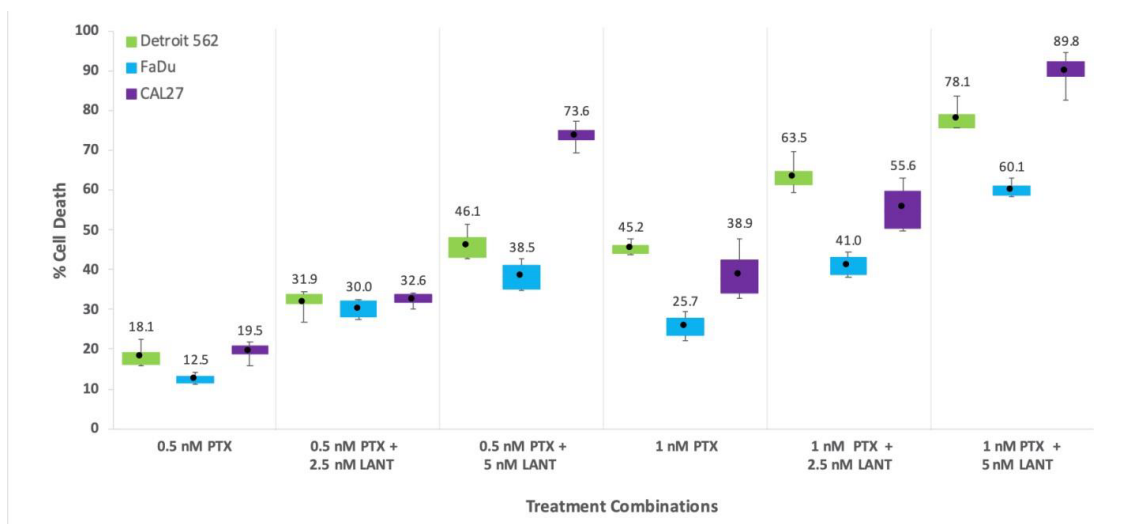


**Figure 4:** Box and whisker plot to display LANT and PTX combination treatment for HNSCC cell lines: Detroit 562 (green bar), FaDu (blue bar), and CAL 27 (purple bar), corresponding to Tables 2 and 3. Boxes (whiskers) indicate variability outside the upper and lower quartiles of  $n=4$  and dots show the mean values of  $n=4$ .

**Table 2:** Summary statistics for PTX monotreatment and LANT combination treatment outcome. Mean, mean percentage; SD, standard deviation; Min, minimum; Max, maximum; and N, number observations of cell death induced for six treatment groups for three HNSCC cell lines, Detroit 562, FaDu and CAL 27.

Cell line	Statistic	Treatment combination					
		0.5 nM PTX	0.5 nM PTX + 2.5 nM LANT	0.5 nM PTX + 5 nM LANT	1 nM PTX	1 nM PTX + 2.5 nM LANT	1 nM PTX + 5 nM LANT
Detroit 562	Mean	18.14	31.90	46.07	45.23	63.47	78.10
	SD	3.03	3.44	4.09	1.76	4.33	3.78
	Min	15.73	26.86	42.78	43.74	59.46	75.74
	Max	22.48	34.58	51.51	47.71	69.59	83.67
	Obs	4	4	4	4	4	4
FaDu	Mean	12.46	30.05	38.52	25.67	40.98	60.12
	SD	1.27	2.46	3.89	3.26	3.05	2.06
	Min	11.39	27.55	35.18	22.07	38.01	58.32
	Max	14.16	32.35	42.90	29.39	44.54	62.86
	Obs	4	4	4	4	4	4
CAL 27	Mean	19.50	32.56	73.64	38.92	55.56	89.78
	SD	2.46	1.83	3.32	6.74	6.33	5.12
	Min	15.99	30.09	69.34	32.68	49.86	82.53
	Max	21.72	34.17	77.42	47.63	63.02	94.55
	Obs	4	4	4	4	4	4

The LMM regression Post-Hoc test outcomes were similar across all three cell lines, and the results are summarized in Table 3. The Post-Hoc analyses results for all three cell lines indicated statistically significant differences ( $p < 0.05$ ) in the majority of comparisons of interest between the six treatment groups.

The most effective combination with the most notable increase in cell death over its corresponding PTX monotreatment was 0.5 nM PTX+5 nM LANT, with approximately 2.5-, 3.1-, and 3.8-fold greater cell death than 0.5 nM PTX monotreatment for Detroit 562, FaDu, and CAL 27, respectively (Table 2).

Overall, the combination of PTX and LANT was significantly more effective than the corresponding PTX monotreatment. The highest increase in cell death over its corresponding PTX monotreatment was 1 nM PTX+5 nM LANT, with approximately 78.1%, 60.1%, and 89.8% for Detroit 562, FaDu, and CAL 27, respectively. Furthermore, other combinations (0.5 nM PTX+2.5 nM LANT;

0.5 nM PTX+5 nM LANT; 1 nM PTX + 2.5 nM LANT; and 1 nM PTX+5 nM LANT) were also significantly more effective at inducing cell death in all three cell lines than the corresponding PTX monotreatment (0.5 nM PTX or 1 nM PTX).

As summarized in Table 3, there was only one comparison (of 15 comparisons) for each Detroit 562 and CAL 27 that did not exhibit statistically significant differences in their efficacy: for Detroit 562, 0.5 nM PTX+5 nM LANT was not significantly different from 1 nM PTX and for CAL 27, 0.5 nM PTX+2.5 nM LANT was not significantly different from 1 nM PTX. For FaDu, two comparisons showed no significant difference: 0.5 nM PTX+2.5 nM LANT vs. 1 nM PTX and 1 nM PTX+2.5 nM LANT vs. 0.5 nM PTX+5 nM LANT.

The 4PL model equation was used to determine the synergistic therapeutic efficacy of the combination treatment and the percentage of PTX dose reduction. The cell death percentages

**Table 3:** Comparing the efficacy of each PTX monotreatment and combination treatment groups by the Linear Mixed Model (LMM) regression Post-Hoc tests with Bonferroni correction for Detroit 562, FaDu, and CAL 27 cell lines. For treatment group comparison, the first column was more effective than the second column by the mean difference amount; Mean Diff, Mean Difference=first column - second column; \* $p<0.0001$ ; † $p<0.005$ ; ‡ $p<0.05$ .

Treatment group comparison (First Column vs. Second Column)		Detroit 562		FaDu		CAL 27	
		Mean Diff	p-value	Mean Diff	p-value	Mean Diff	p-value
0.5 nM PTX+2.5 nM LANT	0.5 nM PTX	13.8	<0.0001*	17.6	<0.0001*	13.1	<0.0001*
0.5 nM PTX+5 nM LANT	0.5 nM PTX	27.9	<0.0001*	26.1	<0.0001*	54.1	<0.0001*
1 nM PTX+2.5 nM LANT	0.5 nM PTX	45.3	<0.0001*	28.5	<0.0001*	36.1	<0.0001*
1 nM PTX + 5 nM LANT	0.5 nM PTX	60.0	<0.0001*	47.7	<0.0001*	70.3	<0.0001*
0.5 nM PTX + 2.5 nM LANT	1 nM PTX	-13.3	<0.0001*	4.376	0.9999	-6.36	0.299
0.5 nM PTX + 5 nM LANT	1 nM PTX	0.848	0.9999	12.85	<0.0001*	34.72	<0.0001*
1 nM PTX + 2.5 nM LANT	1 nM PTX	18.2	<0.0001*	15.3	<0.0001*	16.6	<0.0001*
1 nM PTX + 5 nM LANT	1 nM PTX	32.9	<0.0001*	34.4	<0.0001*	50.9	<0.0001*
1 nM PTX	0.5 nM PTX	27.1	<0.0001*	13.2	<0.0001*	19.4	<0.0001*
0.5 nM PTX + 5 nM LANT	0.5 nM PTX + 2.5 nM LANT	14.2	<0.0001*	8.47	0.035†	41.1	<0.0001*
1 nM PTX + 2.5 nM LANT	0.5 nM PTX + 2.5 nM LANT	31.6	<0.0001*	10.9	0.002§	23.0	<0.0001*
1 nM PTX + 5 nM LANT	0.5 nM PTX + 2.5 nM LANT	46.2	<0.0001*	30.1	<0.0001*	57.2	<0.0001*
1 nM PTX + 2.5 nM LANT	0.5 nM PTX + 5 nM LANT	17.4	<0.0001*	2.46	0.9999	-18.08	<0.0001*
1 nM PTX + 5 nM LANT	0.5 nM PTX + 5 nM LANT	32.0	<0.0001*	21.6	<0.0001*	16.1	<0.0001*
1 nM PTX + 5 nM LANT	1 nM PTX + 2.5 nM LANT	14.6	<0.0001*	19.1	<0.0001*	34.2	<0.0001*

**Table 4:** PTX dose reduction percentage by PTX+LANT combination treatments. The bold indicates the combination treatment resulting in the highest percentage of PTX dose reduction for each cell line.

Cell line	Outcome	Treatment combination			
		0.5 nM PTX+2.5 nM LANT	0.5 nM PTX+5 nM LANT	1 nM PTX+2.5 nM LANT	1 nM PTX+5 nM LANT
Detroit 562	Cell death (%) in combo	31.9	46.1	63.5	78.1
	Est. conc. (nM) of PTX mono to obtain the same % cell death	1.2	2.0	3.7	7.1
	PTX dose reduction (%)	57.8	74.8	72.9	86.0
FaDu	Cell death (%) in combo	30.0	38.5	41.0	60.1
	Est. conc. (nM) of PTX mono to obtain the same % cell death	2.0	2.6	2.8	4.6
	PTX dose reduction (%)	75.5	80.8	64.0	78.1
CAL 27	Cell death (%) in combo	32.6	73.6	55.6	89.8
	Est. conc. (nM) of PTX mono to obtain the same % cell death	0.7	3.1	1.6	7.6
	PTX dose reduction (%)	30.9	84.1	38.0	86.8

induced by the 4 combinations of PTX+LANT (0.5 nM or 1 nM PTX+2.5 nM or 5 nM LANT) were evaluated. The dose of PTX monotreatment necessary to achieve the same cell death percentage as the corresponding PTX used the combination treatments was determined. The reduction in dose was derived using cell death percentage as the commonality (Table 4).

Both the 0.5 nM PTX+5 nM LANT combination treatment and the 1 nM PTX+5 nM LANT combination treatment resulted in greater than 75% of PTX dose reduction for all 3 cell lines. The 1 nM PTX+5 nM LANT combination treatment resulted in the highest percentage of PTX dose reduction for Detroit 562 and CAL 27: 86.0% and 86.8% respectively, while the 0.5 nM PTX+5 nM LANT combination treatment resulted in the highest percentage of PTX dose reduction for FaDu: 80.8%. With CAL 27 cell line, for example, 7.6 nM of PTX monotreatment is required to achieve the same 89.8% cell death as the 1 nM PTX when used in the combination treatment (1 nM PTX+5 nM LANT), demonstrating an 86.8% PTX dose reduction.

## DISCUSSION

Viable approaches using combination, adjuvant, and neoadjuvant therapies have been used to overcome the current challenges experienced by cancer patients who cannot receive or tolerate the standard of care chemotherapy regimens. These patient-centered solutions reduce the standard drug dosage administered, reducing toxicity, side effects, and poor prognoses. As one of the standard chemotherapies for HNSCC, PTX has shown promise to decrease toxicity and side effects at lower doses when combined with other therapeutic interventions. Clinically, it has been reported that PTX combined with other chemotherapeutic drugs demonstrate dose reduction while maintaining or improving efficacy, especially when utilizing an altered dosing schedule. These options include a wide range of PTX combination therapies including that with cisplatin, 5-fluorouracil, cetuximab, panitumumab, buparlisib, and carboplatin [31-36]. For example, PTX paired with carboplatin was shown to be a safe and effective first-line therapy alternative for

HNSCC patients who cannot tolerate more aggressive treatment options. Pêtre et al. found that 80 mg/m<sup>2</sup> of PTX administered weekly with carboplatin improved efficacy and overall survival when compared with the standard therapy, cetuximab, cisplatin and 5-fluorouracil combination [35]. When pairing PTX and carboplatin combination with adjuvant radiochemotherapy in HNSCC patients, PTX dosage could be even further reduced to 40 mg/m<sup>2</sup> administered weekly [36]. Fewer grade 3 and 4 toxicities were recorded for the 40 mg/m<sup>2</sup> PTX-carbolplatin-radiochemotherapy study than the 80 mg/m<sup>2</sup> PTX-carboplatin regimen.

In recent pre- and early-clinical studies, combining PTX with various unconventional interventions, like nanomedicines and therapeutic nanotechnologies, has promise for PTX dose reduction, increased efficacy, and improved delivery [19,37-44]. New developments of PTX-conjugated gold nanoparticles showed ability to solve PTX insolubility, deliver nucleic acid for gene therapy, target specifically cancer cells, modulate drug release, and amplify PTT [45-53]. For example, Peralta et al. reported that utilization of hybrid PTX and AuNR-loaded human serum albumin nanoparticles in PTT enhanced PTX monotreatment efficacy by 14% *in vitro*, demonstrating ~94% cell death with only 20 µg/mL of PTX [53].

We present a combination therapy in this study that utilizes a non-conjugated, injectable PTX treatment followed by LANT as a PTT. Our platform was designed to lower the effective drug dosage and thereby potentially minimize the unintended side effects of PTX. Combining PTX and LANT is synergistic thermal ablative local therapy, not a drug delivery system. In our previous study, LANT monotreatment induced greater than 95% cell death ( $p < 0.0001$ ) *in vitro* and greater than 95% xenograft tumor regression *in vivo* ( $p < 0.0001$ ) in HNSCC [26]. In this present study, combining PTX with LANT increased the percentage of cell death by up to 3.8-fold and the efficacy of cell death up to 54.1% more than PTX monotreatment. The most effective treatment combination, 1 nM PTX+5 nM LANT, demonstrated an 86.8% dose reduction in CAL 27, compared to the 7.6 nM of PTX monotreatment required to achieve the same 89.8% cell death. These results suggest that a lower PTX dose may be used in combination with LANT to achieve the same therapeutic efficacy as higher doses of PTX monotreatment. The direct translation and correlation this *in vitro* concentration to an animal or human dose is not yet a process that is delineated in the literature. However, if the same 86.8% dose reduction could be applied to the standard human PTX dose schedule, future LANT studies may lead to the reduction of the standard clinical dose of PTX from 175 mg/m<sup>2</sup> to 23.1 mg/m<sup>2</sup>.

Our results suggest that LANT may improve the therapeutic efficiency of low doses of PTX, which could result in fewer side effects for cancer patients and improve patient outcomes. Consequently, the combination of LANT and PTX *in vitro* implies the possibility of a much-needed reduction in the morbidity and mortality of a variety of cancers. LANT may also reduce the effective dose and enhance the therapeutic efficacy of other chemotherapeutic drugs in addition to PTX. Our future studies will include validation of these findings *in vivo*. Further, our findings may extend to a variety of other cancer types, and lead to the development of new adjuvant therapeutic interventions, incorporating other metallic-based nanoparticle, such as other gold, silver, platinum, and iron nanoparticles. Consequently, future studies will be needed to determine the advantages of combining LANT with other treatment options and the potential for improving the treatment experience for patients with a variety of cancer types.

## ACKNOWLEDGMENTS

All authors listed made substantial, direct, and intellectual contributions to the work discussed in this manuscript. HNG was responsible for study conception and design and developed the LANT technology and protocols. GYL was responsible for data acquisition and performed the experiments. MM was responsible for statistical analysis. HNG, GYL, MM, and MBC performed data analysis, designed, drafted and revised the manuscript. All authors analyzed the data, read and approved the final manuscript. The authors would also like to thank the supporters and volunteers at the Ora Lee Smith Cancer Research Foundation for their endeavors to translate LANT from bench to bedside, while making it affordable and accessible.

## FUNDING

The study was primarily supported by Award Number I01BX007080 from the Biomedical Laboratory Research and Development Service of the VA Office of Research and Development and partially supported by the National Center for Advancing Translational Sciences of the National Institutes of Health under Award Number UL1TR000454 and National Cancer Institute awards: P30CA013148, P50CA098252, U54CA118938, U54CA118623, and U54CA118948. The contents of this article are solely the responsibility of the authors and do not necessarily represent the official views of the funding agency, VA or NIH.

## DISCLOSURE STATEMENT

Conflict of Interest: None to report.

## REFERENCES

- Zhang Z, Mei L, Feng SS. Paclitaxel drug delivery systems. *Expert Opin Drug Deliv.* 2013;10(3):325-340.
- Weaver BA. How Taxol/paclitaxel kills cancer cells. *Mol Biol Cell.* 2014;25(18):2677-2681.
- Marupudi NI, Han JE, Li KW, Renard VM, Tyler BM, Brem H. Paclitaxel: A review of adverse toxicities and novel delivery strategies. *Expert Opin Drug Saf.* 2007;6(5):609-621.
- Siegel R, Naishadham D, Jemal A. Cancer statistics, 2013. *CA Cancer J Clin.* 2013;63(1):11-30.
- Bray F, Ferlay J, Soerjomataram I, Siegel RL, Torre LA, Jemal A. Global cancer statistics 2018: GLOBOCAN estimates of incidence and mortality worldwide for 36 cancers in 185 countries. *CA Cancer J Clin.* 2018;68(6):394-424.
- Locally Advanced Squamous Carcinoma of the Head and Neck. World Health Organization. Published 2014.
- [https://www.who.int/selection\\_medicines/committees/expert/20/applications/HeadNeck.pdf](https://www.who.int/selection_medicines/committees/expert/20/applications/HeadNeck.pdf). Accessed on Dec 17, 2020.
- Marur S, Forastiere AA. Head and neck squamous cell carcinoma: update on epidemiology, diagnosis, and treatment. *Mayo Clin Proc.* 2016;91(3):386-396.
- Alsahafi E, Begg K, Amelio I, Raulf N, Lucarelli P, Sauter T, et al. Clinical update on head and neck cancer: molecular biology and ongoing challenges. *Cell Death Dis.* 2019;10(8):540.
- Wo SK, Li CR, Zuo Z. Evaluation of cellular uptake of three paclitaxel formulations in cancer cells. Poster abstracts (P96). *Drug Metab Rev.* 2011;43(sup2):83.

11. Scripture CD, Figg WD, Sparreboom A. Peripheral neuropathy induced by paclitaxel: Recent insights and future perspectives. *Curr Neuropharmacol*. 2006;4(2):165-172.
12. Boyette-Davis JA, Cata JP, Driver LC, Novy DM, Bruel BM, Mooring DL, et al. Persistent chemoneuropathy in patients receiving the plant alkaloids paclitaxel and vincristine. *Cancer Chemother Pharmacol*. 2013;71(3):619-626.
13. Chemotherapy-linked neuropathy can affect balance, gait even years after treatment ends. *Breastcancer.org*. Published June 15, 2017. <https://www.breastcancer.org/research-news/neuropathy-effects-last-years-after-tx>. Accessed Nov 4, 2020.
14. Enokida T, Okano S, Fujisawa T, Ueda Y, Uozumi S, Tahara M. Paclitaxel plus cetuximab as 1st line chemotherapy in platinum-based chemoradiotherapy-refractory patients with squamous cell carcinoma of the head and neck. *Front Oncol*. 2018;8:339.
15. Gonzalez-Angulo AM, Hortobagyi GN. Optimal schedule of paclitaxel: Weekly is better. *J Clin Oncol*. 2008;26(10):1585-1587.
16. Soulières D, Faivre S, Mesía R, Remenár É, Li SH, Karpenko A, et al. Buparlisib and paclitaxel in patients with platinum-pretreated recurrent or metastatic squamous cell carcinoma of the head and neck (BERIL-1): A randomised, double-blind, placebo-controlled phase 2 trial. *Lancet Oncol*. 2017;18(3):323-335.
17. Perez EA. Paclitaxel in breast cancer. *Oncologist*. 1998;3(6):373-389.
18. Taxol® (Paclitaxel) injection label - FDA. Bristol-Myers Squibb Company. Revised April 2011. [https://www.accessdata.fda.gov/drugsatfda\\_docs/label/2011/020262s049lbl.pdf](https://www.accessdata.fda.gov/drugsatfda_docs/label/2011/020262s049lbl.pdf). Accessed Nov 2, 2020.
19. Singla AK, Garg A, Aggarwal D. Paclitaxel and its formulations. *Int J Pharm*. 2002;235(1-2):179-192.
20. Chowdhury P, Nagesh PKB, Hatami E, Wagh S, Dan N, Tripathi MK, et al. Tannic acid-inspired paclitaxel nanoparticles for enhanced anticancer effects in breast cancer cells. *J Colloid Interface Sci*. 2019;535:133-148.
21. Nehate C, Jain S, Saneja A, Khare V, Alam N, Dubey RD, et al. Paclitaxel formulations: challenges and novel delivery options. *Curr Drug Deliv*. 2014;11(6):666-686.
22. Tran PHL, Duan W, Lee B, Tran TTD. Nanogels for skin cancer therapy via transdermal delivery: current designs. *Curr Drug Metab*. 2019;20(7):575-582.
23. Her S, Jaffray DA, Allen C. Gold nanoparticles for applications in cancer radiotherapy: Mechanisms and recent advancements. *Adv Drug Deliv Rev*. 2017;15: 84-101.
24. Choi YJ, Kim YJ, Lee JW, Lee Y, Lee S, Lim YB, et al. Cytotoxicity and genotoxicity induced by photothermal effects of colloidal gold nanorods. *J Nanosci Nanotechnol*. 2013;13(6):4437-4445.
25. Zhou B, Song J, Wang M, Wang X, Wang J, Howard EW, et al. BSA-bioinspired gold nanorods loaded with immunoadjuvant for treatment of melanoma by combined photothermal therapy and immunotherapy. *Nanoscale*. 2018;10(46):21640-21647.
26. Popp MK, Oubou I, Shepherd C, Nager Z, Anderson C, Pagliaro L. Photothermal therapy using gold nanorods and near-infrared light in a murine melanoma model increases survival and decreases tumor volume. *J Nanomater*. 2014;8.
27. Green HN, Crockett SD, Martyshkin DV, Singh KP, Grizzle WE, Rosenthal EL, et al. A histological evaluation and in vivo assessment of intratumoral near infrared photothermalnanotherapy-induced tumor regression. *Int J Nanomed*. 2014;9:5093-5102.
28. Green HN, Martyshkin DV, Rosenthal EL, Mirov S. A minimally invasive multifunctional nanoscale system for selective targeting, imaging, and NIR photothermal therapy of malignant tumors. In: *Reporters, Markers, Dyes, Nanoparticles, and Molecular Probes for Biomedical Applications III*. Vol 7910. International Society for Optics and Photonics; 2011:79100B.
29. Link S, El-Sayed MA. Simulation of the optical absorption spectra of gold nanorods as a function of their aspect ratio and the effect of the medium dielectric constant. *J Phys Chem B*. 2005;109:10531-10532.
30. Sebaugh JL. Guidelines for accurate EC50/IC50 estimation. *Pharm Stat*. 2011;10(2):128-134.
31. Long JS. *Regression Models for Categorical and Limited Dependent Variables*. 1st ed. London, UK: Sage Publications, Inc.; 1997.
32. Zhou L, Xu S, Yin W, Lin Y, Du Y, Jiang Y, et al. Weekly paclitaxel and cisplatin as neoadjuvant chemotherapy with locally advanced breast cancer: A prospective, single arm, phase II study. *Oncotarget*. 2017;8:79305-79314.
33. Wanebo H, Lee J, Burtress B, Ridge JA, Ghebremichael M, Spencer SA, et al. Induction cetuximab, paclitaxel, and carboplatin followed by chemoradiation with cetuximab, paclitaxel, and carboplatin for stage III/IV head and neck squamous cancer: A phase II ECOG-ACRIN trial. *Annals of Oncology*. 2014;25(10): 2036-2041.
34. Morillo I, Mesía R, Klain J, Fernández S, Martínez-Galán J, Borgoñon M, et al. Phase II study of panitumumab and paclitaxel as first-line treatment in recurrent or metastatic head and neck cancer. *Oral Oncol*. 2016;62: 54-49.
35. Soulières D, Faivre S, Mesía R, Remenár É, Li SH, Karpenko A, et al. Buparlisib and paclitaxel in patients with platinum-pretreated recurrent or metastatic squamous cell carcinoma of the head and neck (BERIL-1): A randomised, double-blind, placebo-controlled phase 2 trial. *Lancet Oncol*. 2017;18(3):323-335.
36. Pêtre A, Dalban C, Karabajakian A, Neidhardt EM, Roux PE, Poupard M, et al. Carboplatin in combination with weekly paclitaxel as first-line therapy in patients with recurrent/metastatic head and neck squamous cell carcinoma unfit to EXTREME schedule. *Oncotarget*. 2018;9(31):22038-22046.
37. Maring S, Elsayad K, Stenner M, Rudack C, Haverkamp U, Rehkämper J, et al. Efficacy of carboplatin/paclitaxel-based radiochemotherapy in locally advanced squamous cell carcinoma of head and neck. *Oncol Res Treat*. 2018;41:736-742.
38. Suri SS, Fenniri H, Singh B. Nanotechnology-based drug delivery systems. *J Occup Med Toxicol*. 2007;2:16.
39. Wang J, Sui M, Fan W. Nanoparticles for tumor targeted therapies and their pharmacokinetics. *Curr Drug Metab*. 2010;11:129-141.
40. Wang F, Porter M, Konstantopoulos A, Zhang P, Cui H. Preclinical development of drug delivery systems for paclitaxel-based cancer chemotherapy. *J Control Release*. 2017;267:100-118.
41. Buyukkoroglu G, Senel B, Basaran E, Gezgin S. Development of paclitaxel-loaded liposomal systems with anti-her2 antibody for targeted therapy. *Trop J Pharm Res*. 2016;15:895-903.
42. Liu YY, Ran R, Chen JT, Kuang Q, Tang J, Mei L, et al. Paclitaxel loaded liposomes decorated with a multifunctional tandem peptide for glioma targeting. *Biomaterials*. 2014;35:4835-4847.
43. Pandey V, Gajbhiye KR, Soni V. Lactoferrin-appended solid lipid nanoparticles of paclitaxel for effective management of bronchogenic carcinoma. *Drug Deliv*. 2015;22:199-205.
44. Gao NS, Chen ZH, Xiao XJ, Ruan C, Mei L, Liu Z, et al. Surface modification of paclitaxel-loaded tri-block copolymer PLGA-b-PEG-b-PLGA nanoparticles with protamine for liver cancer therapy. *J Nanopart Res*. 2015;17.
45. Ma P, Mumper RJ. Paclitaxel nano-delivery systems: A comprehensive



- review. *J Nanomed Nanotechnol.* 2013;4(2):1000164.
46. Banstola A, Pham TT, Jeong JH, Yook S. Polydopamine-tailored paclitaxel-loaded polymeric microspheres with adhered NIR-controllable gold nanoparticles for chemophototherapy of pancreatic cancer. *Drug Deliv.* 2019;26:629-640.
47. Bao QY, Zhang N, Geng DD, Xue JW, Merritt M, Zhang C, et al. The enhanced longevity and liver targetability of Paclitaxel by hybrid liposomes encapsulating paclitaxel-conjugated gold nanoparticles. *Int J Pharm.* 2014;477:408-415.
48. Ding Y, Zhou YY, Chen H, Geng DD, Wu DY, Hong J, et al. The performance of thiol-terminated PEG-paclitaxel-conjugated gold nanoparticles. *Biomaterials.* 2013;34:10217-10227.
49. Vemuri SK, Banala RR, Mukherjee S, Uppala P, Gpv S, A V GR, et al. Novel biosynthesized gold nanoparticles as anti-cancer agents against breast cancer: Synthesis, biological evaluation, molecular modelling studies. *Mater Sci Eng C Mater Biol Appl.* 2019;99:417-429.
50. Li F, Zhou XF, Zhou HY, Jia J, Li L, Zhai S, et al. Reducing both PGP overexpression and drug efflux with anti-cancer gold-paclitaxel nanoconjugates. *PLoS One.* 2016;11:e0160042.
51. Heo DN, Yang DH, Moon HJ, Lee JB, Bae MS, Lee SC, et al. Gold nanoparticles surface-functionalized with paclitaxel drug and biotin receptor as theranostic agents for cancer therapy. *Biomaterial.* 2012;33:856-866.
52. Paciotti GF, Zhao JL, Cao SG, Brodie PJ, Tamarkin L, Huhta M, et al. Synthesis and evaluation of paclitaxel-loaded gold nanoparticles for tumor-targeted drug delivery. *Bioconjug Chem.* 2016;27:2646-2657.
53. Wang Z, Dong J, Zhao Q, Ying Y, Zhang L, Zou J, et al. Gold nanoparticle-mediated delivery of paclitaxel and nucleic acids for cancer therapy (Review). *Mol Med Rep.* 2020;22:4475-4484.
54. Peralta DV, Heidari Z, Dash S, Tarr MA. Hybrid paclitaxel and gold nanorod-loaded human serum albumin nanoparticles for simultaneous chemotherapeutic and photothermal therapy on 4T1 breast cancer cells. *ACS Appl Mater Interfaces.* 2015;7(13):7101-11.